Single-Domain Antibody Theranostics on the Horizon

Weijun Wei[1], Muhsin H. Younis[2], Xiaoli Lan[3,4], Jianjun Liu[1], and Weibo Cai[2]

[1]*Department of Nuclear Medicine, Institute of Clinical Nuclear Medicine, Renji Hospital, Shanghai Jiao Tong University School of Medicine, Shanghai, China;* [2]*Departments of Radiology and Medical Physics, University of Wisconsin−Madison, Madison, Wisconsin;* [3]*Department of Nuclear Medicine, Union Hospital, Tongji Medical College, Huazhong University of Science and Technology Wuhan, China; and* [4]*Hubei Key Laboratory of Molecular Imaging Wuhan, China*

Single-domain antibody (sdAb) is among the most promising vectors for developing molecular imaging tracers. Several sdAb tracers targeting human epidermal growth factor receptor 2 or programmed death ligand 1 have entered clinical practice. However, radiolabeled single-valent sdAbs generally have high kidney retention, limiting their therapeutic applications. Therefore, engineering strategies such as PEGylation or incorporation of renal cleavable linkers can be adapted to improve pharmacokinetics and reduce kidney retention. In this Focus on Molecular Imaging review, we try to summarize the latest developments in sdAb-derived agents and propose potential strategies that can be used to improve the theranostic value of radiolabeled sdAbs.

Key Words: nanobody; immuno-PET; radiopharmaceuticals; theranostics; cancer

J Nucl Med 2022; 63:1475–1479
DOI: 10.2967/jnumed.122.263907

The term *molecular imaging* has been well defined as the "visualization, characterization, and measurement of biological processes at the molecular and cellular levels in humans and other living systems" (*1*). With the increasingly approved therapeutic antibodies and commercial supply of long-lived radionuclides such as ^{89}Zr and ^{64}Cu, immuno-PET imaging with radiolabeled monoclonal antibodies has fulfilled some of the tasks by visualizing target expression and guiding antibody development (*2*). Safety profiles, easy access, availability in large amounts, and robust labeling protocols are natural advantages of developing monoclonal antibody–based tracers, but slow clearance, less optimal tumor-to-background ratios, poor penetration in tumor interstitium, and noticeable radiation dose are practical considerations hindering their routine clinical use. Additionally, imaging at several time points in a week is inconvenient for patients.

Immuno-PET imaging with radiolabeled single-domain antibodies (sdAbs) has rapidly evolved (*3,4*). There are 2 major types of sdAbs, one isolated from human antibody repertoires and another from camelid heavy-chain–only antibodies. But sdAbs can also be engineered from sharks. As the smallest antibody fragment, with a molecular size of 15 kDa, variable domain of the heavy chain of heavy-chain–only antibodies (VHH, or Nanobody; Ablynx) is characterized by high affinity, high stability, efficient extravasation, and, most importantly, ease of engineering. Herein, we present the latest progress in sdAb theranostics and lay out future innovation and translation perspectives.

AGENTS TARGETING BIOMARKERS ON TUMOR CELLS

Human Epidermal Growth Factor Receptor 2 (HER2)

HER2 is among the most thoroughly explored receptor tyrosine kinases for molecular imaging. Currently, 2 HER2-specific sdAb tracers have been translated for clinical use. ^{68}Ga-NOTA-2Rs15d was preclinically investigated in 2013 (*5*), followed by successful clinical translation in 2016 (*6*). More recently, the same group developed ^{131}I-4-guanidinomethyl-3-iodobenzoate (GMIB)-anti-HER2-VHH1 (*7*), in which ^{131}I was attached to the VHH1 (2Rs15d) via the linker *N*-succinimidyl-GMIB (SGMIB). Accumulation of ^{131}I-GMIB-anti-HER2-VHH1 was observed in patients with metastatic breast cancers (*8*). A low dose (46 ± 28 MBq for healthy subjects and 64 ± 46 MBq for patients) was administered in the study. A phase I/II dose-expansion study to evaluate the safety, tolerability, dosimetry, and efficacy of ^{131}I-GMIB-anti-HER2-VHH1 is currently ongoing (NCT04467515). Increased tumor uptake and faster clearance of radioiodinated sdAbs are favored for radioimmunotherapy. Feng et al. recently reported that iso-^{131}I-SGMIB-VHH_1028 exhibited significantly higher tumor uptake and lower kidney accumulation than ^{131}I-SGMIB-2Rs15d (^{131}I-GMIB-anti-HER2-VHH1). More importantly, the theranostic agent significantly suppressed tumor growth and prolonged survival (*9*).

Meanwhile, Zhao et al. developed another sdAb tracer, ^{99m}Tc-NM-02, and conducted an early phase I study (NCT04040686) enrolling 10 patients with breast cancer (*10*). After bolus injection of 458 ± 37 MBq of ^{99m}Tc-NM-02 (100 μg of NM-02), no adverse effects were reported and tumor uptake of ^{99m}Tc-NM-02 correlated well with HER2 expression (Fig. 1). Traditionally, *N*-succinimidyl-4-^{18}F-fluorobenzoate, a nonresidualizing prosthetic agent, was used to develop the HER2-specific probe ^{18}F-RL-I-5F7, which imaged HER2 status, but the diagnostic efficacy was compromised by a problematic renal background (*11,12*). Residualizing prosthetic agents for ^{18}F labeling are favored for improving the tumor trap of the tracers. By migrating high temperature and organic solvents, which may denature the sdAbs, click chemistry reactions are increasingly used to facilitate ^{18}F labeling. Zhou et al. harnessed a tetrazine/*trans*-cyclooctene inverse electron-demand Diels-Alder cycloaddition reaction and incorporated a renal brush border enzyme-cleavable linker and a polyethylene glycol (PEG) 4 chain between ^{18}F and 5F7 in developing ^{18}F-5F7GGC (*13*), which yielded high retention in the tumor with very little background activity. Several clinical trials are investigating either the diagnostic (NCT04591652, NCT03331601, and NCT03924466) or the

Received Apr. 17, 2022; revision accepted Jul. 7, 2022.
For correspondence or reprints, contact Jianjun Liu (nuclearj@163.com) or Weibo Cai (wcai@uwhealth.org).
Published online Jul. 14, 2022.

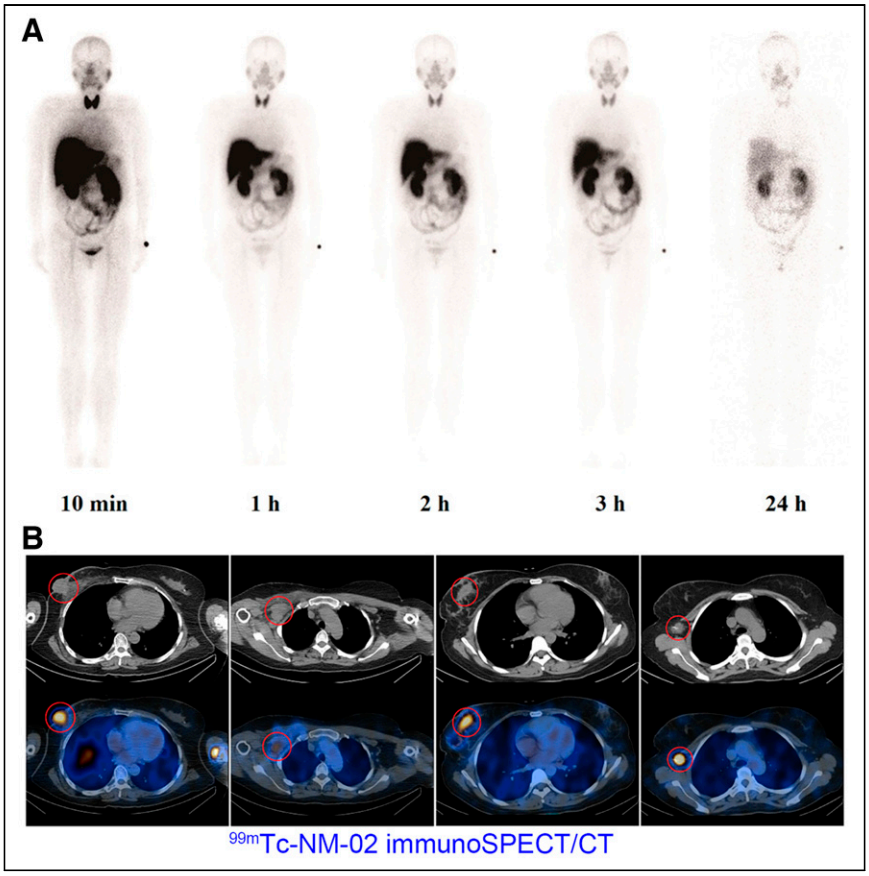

FIGURE 1. ^{99m}Tc-NM-02 immuno-SPECT/CT imaging of breast cancers. (A) Whole-body SPECT images at different time points (10 min, 1 h, 2 h, 3 h, and 24 h) after injection of radiotracer. (B) Varying uptake patterns in patients with breast cancer. From left to right: heterogeneous uptake in primary tumor and in metastatic lymph node in patient with HER2 3+ breast cancer, and homogeneous uptake in primary tumor and in metastatic lymph node in another patient with HER2 3+ breast cancer. Primary and metastatic tumors are indicated by red circles. (Reprinted from (*10*).)

theranostic (NCT04467515) value of radiolabeled HER2-targeting sdAbs in HER2-overexpressing solid tumors.

Epidermal Growth Factor Receptor (EGFR)

EGFR is another receptor tyrosine kinase involved in cancer development and progression. Although monoclonal antibody and small-molecule–based tracers have entered clinical translation, no sdAb-based tracers have achieved clinical translation so far. 7C12 and 7D12 are the most widely used EGFR-targeting sdAbs in molecular imaging. Vosjan et al. synthesized ^{89}Zr-Df-Bz-NCS-7D12 and reported the diagnostic value in A431 tumor–bearing mice (*14*). The generally introduced His_6 tag could be used for site-specific labeling using $[^{99m}Tc(CO)_3]^+$. ^{99m}Tc-7C12 and ^{99m}Tc-7D12 were labeled with ^{99m}Tc at their His_6 tag tails. ^{99m}Tc-7C12 showed a higher tumor uptake, higher kidney uptake, and lower liver uptake than ^{99m}Tc-7D12 (*15*). D10, another anti-EGFR sdAb, was also site-specifically labeled with $[^{99m}Tc(CO)_3]^+$, and ^{99m}Tc-D10 detected small tumors more efficiently than ^{99m}Tc-cetuximab (*16*).

Programmed Death Ligand 1 (PD-L1)

PD-L1 is an immune checkpoint that interacts with the receptor programmed death 1 on T cells, inhibiting T-cell activation and suppressing antitumor immunity. Immune checkpoint blockade with antibodies targeting the programmed death 1/PD-L1 axis has prolonged survival in cancer patients. However, reliable biomarkers that can predict the responses are lacking. PD-L1 status revealed by immunohistochemistry is not always associated with treatment efficacy (*17*), possibly because of inherent artifacts of immunohistochemistry such as tissue sampling errors and inequivalent interpretation of the staining results (*18*).

Xing et al. developed the sdAb-derived ^{99m}Tc-NM-01 and reported the physiologic uptake of the tracer in the liver, spleen, and, to a lesser extent, bone marrow and lungs. The translational study showed intratumoral and intertumoral heterogeneity of PD-L1 expression and a good correlation between the SPECT signal and immunohistochemistry results (*19*). Although ^{99m}Tc-labeled tracers have long half-lives and good availabilities, the low spatial resolution and lack of quantitation with SPECT are potential challenges in quantifying PD-L1. To this end, ^{68}Ga-labeled sdAb tracers targeting PD-L1 have been developed (*20–22*). Although site-specific labeling yields well-defined and homogeneous conjugates, there were no differences in binding affinities and diagnostic efficacies between the site-specifically and randomly labeled sdAb tracers (*22*). KN035 is an engineered sdAb derivative with a molecular weight of 79.6 kDa. Li et al. developed ^{89}Zr-Df-KN035 and reported the diagnostic efficacy in glioma xenografts and the circulation profiles in nonhuman primates (Supplemental Fig. 1; supplemental materials are available at http://jnm.snmjournals.org) (*23*). An ongoing clinical trial is evaluating the safety and biodistribution of ^{89}Zr-Df-KN035 in patients with PD-L1−positive solid tumors (NCT04977128). Notably, KN035, with a commercial name of envafolimab (Alphamab Oncology), has been approved for treating late-stage solid tumors in China and late-stage biliary tract carcinoma and soft-tissue sarcoma in the United States.

Biomarkers for Multiple Myelomas

CD38 (*12,24,25*), B-cell maturation antigen (*26*), CS1 (*27,28*), and paraprotein (*29*) are promising targets exploited for molecular imaging of multiple myeloma. ^{68}Ga-NOTA-Nb1053 is the first-generation CD38-specific sdAb tracer that realized precise delineation of disseminated multiple myeloma in preclinical settings (Fig. 2A). And the tracer had advantages over ^{18}F-FDG in terms of diagnostic contrast and specificity (Fig. 2B) (*12*). By taking advantage of biorthogonal click chemistry (*24*), ^{18}F-Nb1053 was further innovated and the diagnostic value was also confirmed in multiple myeloma models (Figs. 2C and 2D). The justification for developing ^{18}F-labeled cousins is that such tracers allow distribution to multiple centers on clinical translation. 2F8 is an sdAb binding to human CD38 independently of daratumumab. A recent work developed ^{99m}Tc-H_6-2F8 and ^{177}Lu-diethylenetriaminepentaacetic acid (DTPA)-2F8 using untagged and tagged 2F8, respectively. Although the former showed a specific uptake facilitating diagnosis of subcutaneous multiple myeloma, the latter at either a

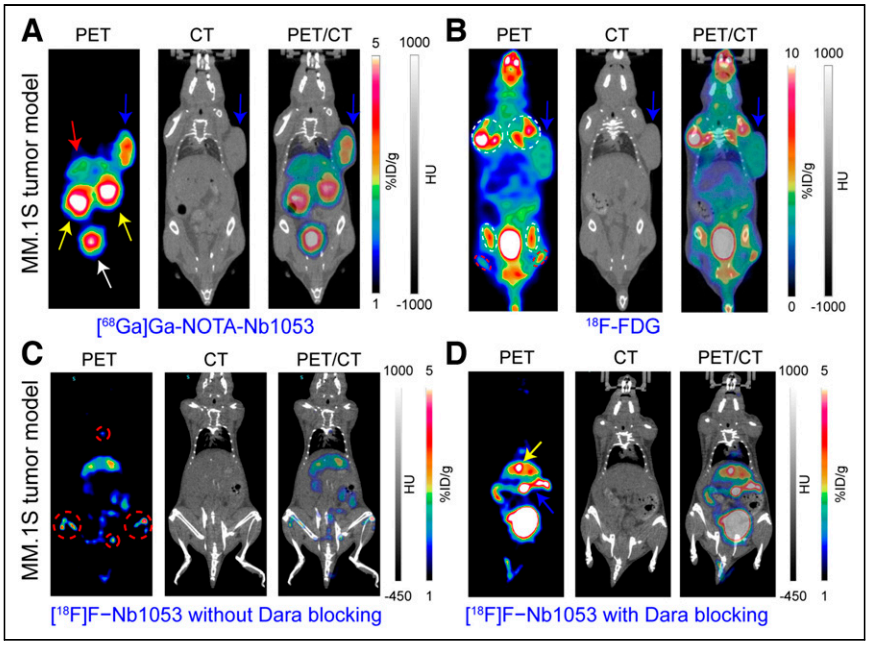

FIGURE 2. Preclinical immuno-PET imaging of multiple myelomas. (A) Immuno-PET imaging with ^{68}Ga-NOTA-Nb1053 delineated subcutaneous MM.1S tumor (blue arrows) with excellent contrast. Unbound tracer was largely excreted from urinary system (kidneys indicated by yellow arrows and bladder by white arrow), and small proportion was catabolized in liver (red arrow). (B) In comparison, PET imaging with ^{18}F-FDG visualized subcutaneous MM.1S tumor (blue arrows) with substantial uptake in normal tissues, such as bone joints (white circles) and muscles (red circles). (C) Immuno-PET imaging with ^{18}F-Nb1053 also clearly outlined involved bones (red circles). (D) In contrast, no obvious ^{18}F-Nb1053 uptake was observed in disseminated MM.1S models that were premedicated with CD38-targeting monoclonal antibody daratumumab. The gallbladder is indicated by the yellow arrow. %ID = percentage injected dose; Dara = daratumumab; HU = Hounsfield units. (Reprinted from (*12,24*).)

high dose (18.5 ± 0.5 MBq) or a low dose (9.3 ± 0.3 MBq) significantly prolonged the median survival of the tumor-bearing mice (*30*). Notably, His_6 tag-free 2F8 was used in constructing ^{177}Lu-DTPA-2F8, and the agent was intravenously given at 3 consecutive times with coinjection of a 150 mg/kg dose of Gelofusine (B. Braun). The formulation matters because a single injection of radiolabeled His_6-tagged sdAb may lead to unacceptable nephrotoxicity. In our experience, bolus injection of 3.7 − 7.4 MBq of ^{177}Lu-labeled His_6-tagged sdAb is still too toxic in preclinical models.

Carbonic Anhydrase IX

Carbonic anhydrase IX catalyzes the conversion of carbon dioxide and water to carbonic acid ($CO_2 + H_2O \rightleftarrows HCO_3^- + H^+$) and is regulated by the von Hippel–Lindau hypoxia-inducible factor axis. Carbonic anhydrase IX is highly expressed in over 95% of clear cell renal cell carcinomas. Radiolabeled sdAb is excreted through the kidneys, detracting from imaging of the primary foci of renal cell carcinoma. Therefore, research on renal cell carcinoma–targeted tracers should focus on solving the impact of renal physiologic excretion and reabsorption. Modifications such as the incorporation of the albumin-binding domain (ABD) may alter the physiologic distribution and improve the diagnostic performance of the tracers (*31*). Recent exquisite work by van Lith et al. adopted the strategy and developed 3 sdAb-derived tracers, that is, ^{111}In-DTPA-B9, low-affinity ^{111}In-DTPA-B9-ABD, and high-affinity ^{111}In-DTPA-B9-ABD (*32*). Their results showed the high affinity and specificity of [^{111}In]In-DTPA-B9 in CAIX-expressing head and neck cancer xenografts. Although low-affinity ^{111}In-DTPA-B9-ABD and high-affinity ^{111}In-DTPA-B9-ABD had increased tumor uptake, the uptake was partially CAIX-independent because the preinjected girentuximab failed to thoroughly reduce the uptake. The authors concluded that the low absolute uptake of ^{111}In-DTPA-B9 and the CAIX-independent uptake of low-affinity ^{111}In-DTPA-B9-ABD and high-affinity ^{111}In-DTPA-B9-ABD preclude these tracers from being used to image hypoxia-induced CAIX expression.

Other Theranostics-Relevant Biomarkers

"One marker fits all" is not realistic from a diagnostic perspective; sdAb tracers targeting other emerging biomarkers are warranted. Epithelial cell adhesion molecule (*33*), glypican 3 (*31*), and dipeptidyl peptidase 6 (*34,35*) are also promising biomarkers exploited for sdAb molecular imaging.

IMAGING TUMOR MICROENVIRONMENT

The tumor microenvironment comprises multiple types of cells, including immune cells, vascular cells, and stromal cells. Given this complexity, it is still challenging to gain a full understanding of the tumor microenvironment and to image it. Although PD-L1−targeted tracers have been discussed in the above section, other representative sdAb tracers targeting tumor microenvironment markers are illustrated in the section.

Intratumoral CD8-positive ($CD8^+$) T cells can selectively detect and eradicate cancer cells. With the progression of the tumors, $CD8^+$ T cells differentiated to a hyporesponsive state with impaired cytotoxic capacity. Although lymphocyte activation gene 3 and programmed death 1 are expressed by both early and late dysfunctional T cells, CD38, CD39, CD101, and TIM3 are expressed predominantly by late dysfunctional T cells. These exhaustion markers are spatiotemporally regulated in the tumor microenvironment. Imaging $CD8^+$ T cells may provide a certain clinical value (*36*). Since the clinical translation of ^{89}Zr-IAB22M2C, a minibody tracer targeting $CD8^+$ T cells (*37,38*), several sdAb-derived tracers have been reported. ^{89}Zr-VHH-X118-PEG_{20}, an sdAb tracer that recognizes mouse CD8a, monitored the antitumor immune responses (*39*). The tracer also tracked immune cell distribution and infiltration in the graft-versus-host disease model (*40*) and in models of influenza A virus (*41*). In the context of immunotherapy, the tracer could depict the infiltration of $CD8^+$ T cells into the tumors and predict the therapeutic responses (*42*). We reported that ^{68}Ga-NOTA-SNA006a, an antihuman CD8α sdAb tracer, could visualize $CD8^+$ tumors and track human $CD8^+$ T cells in humanized models (Supplemental Fig. 2) (*43*). The tracer is currently undergoing clinical translation (NCT05126927).

Secondary to CD8, CD4 is another lineage marker exploited for molecular imaging of T cells. Traenkle et al. generated a series of sdAbs specifically recognizing human CD4 and further labeled the most promising candidate (Nb1) with ^{64}Cu (*44*). Imaging studies showed that ^{64}Cu-CD4-Nb1 $CD4^+$ specifically accumulated in T-cell–rich tissues, including lymph nodes, thymus, liver, and spleen. Lecocq et al. developed an antimouse lymphocyte activation gene

3sdAb tracer and reported the efficacy of the tracer in imaging dynamic lymphocyte activation gene 3 expression on tumor-infiltrating lymphocytes (*45*).

Macrophage mannose receptor (CD206) is an endocytic C-type lectin receptor (175 kDa) highly expressed on macrophages. Nb3.49 is an sdAb cross-reactive for both mouse (dissociation constant, 12 nM) and human (dissociation constant, 1.8 nM) macrophage mannose receptor, and the ^{68}Ga-labeled version is ready for clinical translation (*46,47*). Varasteh et al. further reported the specific uptake of the tracer in atherosclerotic lesions of *APOE*$^{-/-}$ mice on the high-fat diet (*48*). Along with this progress, Devoogdt and coauthors characterized a series of sdAb tracers targeting 3 atherosclerosis-related markers, that is, vascular cell adhesion molecule-1 (*49*), lectinlike oxidized low-density lipoprotein receptor-1 (*50*), and macrophage mannose receptor (*51*), in *APOE*$^{-/-}$mice and atherosclerotic rabbits. The authors reported that a multiparametric study of atherosclerosis using different sdAb tracers was feasible (*52*). Two ongoing clinical trials are exploring the use of ^{68}Ga-NOTA-antimacrophage mannose receptor-VHH2 in patients with cancers, cardiovascular atherosclerosis, or abnormal immune activation (NCT04758650 and NCT04168528). Meanwhile, imaging immune-related cells by targeting other markers is actively explored in preclinical studies (*53*). The most promising sdAb-derived molecular imaging or theranostic agents are listed in Supplemental Table 1.

CHALLENGES AND POTENTIAL SOLUTIONS IN NANOBODY THERANOSTICS

Most of the sdAb agents explored in preclinical models are immunoreactive with human antigens but not with murine antigens, indicating that the preclinical evidence may not reliably mirror clinical imaging outcomes, especially for those targeting immune checkpoints. Therefore, the use of humanized models and nonhuman primates is suggested before moving to clinical trials. Better safety profiles, higher affinity, better tissue penetration, and less immunogenicity are the merits of sdAbs for molecular imaging and endoradiotherapy (*54*). Since sdAbs, monoclonal antibodies, and antibody fragments are biomacromolecules, the production and quality control procedures should follow similar protocols. In other words, sdAbs for translational studies should be produced in current good-manufacturing-practice grade, either in bacteria, yeast, or Chinese hamster ovary systems. The His_6 tag is generally introduced to facilitate purification, but it may potentially cause immunogenicity. Removal of the His_6 tag is preferred at the initial plasma design stage or after purification of the sdAbs.

Notably, the kidney accumulation of radiometal-labeled sdAbs is exceptionally high because of excretion and reabsorption, leading to limited detection efficiency near the kidneys and undesired nephrotoxicity at therapeutic doses. Engineering strategies for migrating such drawbacks should be explored (*55*). Receptors such as megalin and cubilin are involved in the reabsorption of proteins (e.g., albumin and sdAb) in the proximal tubule (*56*). The introduction of cleavable linkers between chelator and sdAb (*57*), PEGylation (*39*), and the development of sdAb fusion proteins (*31,32*) are potential strategies to improve the pharmacokinetics and pharmacodynamics of sdAbs. For instance, the Belgium team has elucidated that the removal of the His_6 tag dramatically reduced kidney retention of radiometal-labeled sdAbs (*5,58*). Moreover, replacement of the His_6 tag with the HEHEHE tag reduced kidney retention of radiometal-labeled Affibody molecules (*59*), but the efficacy needs to be investigated in sdAb-derived agents. Along with the engineering strategies, small molecules (e.g., fructose and maleate), positively charged amino acids (e.g., lysine), and Gelofusine are reported to reduce kidney retention of radiolabeled sdAbs, but these are not general approaches because the efficiencies vary greatly between different tracers (*12,60*).

From a diagnostic perspective, only probes solving unmet clinical demands and having easy accessibility and high reproducibility will carve a niche in the companion diagnostics field. For multiinstitutional studies and commercial development, standardized and kit-based radiolabeling protocols can be innovated and adapted (*61*). In addition to solely imaging the patients for staging and restaging, new tracers may be introduced as companion diagnostics with the same or similar scaffold harnessed for therapeutic applications. Preliminary evidence has shown the promise of sdAb-derived theranostic pairs (*6,8*). In the HER2-targeted theranostic pair, the therapeutic agent ^{131}I-GMIB-anti-HER2-VHH1 was developed using ^{131}I-SGMIB as the prosthetic group, leading to increased stability and lower kidney accumulation of the radiopharmaceutical. The future of nuclear medicine will be continuously shaped by theranostics (*62*); α-particle−labeled sdAbs are also promising therapeutic components in the sdAb theranostic toolbox (*63*).

CONCLUSION

Molecular imaging has substantially improved the diagnosis and treatment of cancers. With further optimization and translation, sdAb theranostics may play important roles in the management of human diseases, especially cancers.

DISCLOSURE

This work was supported in part by the National Key Research and Development Program of China (grant 2020YFA0909000), the National Natural Science Foundation of China (grants 82171972 and 82001878), the Shanghai Rising-Star Program (grant 20QA1406100), the University of Wisconsin–Madison, and the National Institutes of Health (grant P30CA014520). Weibo Cai is a scientific advisor, stockholder, and grantee of Focus-X Therapeutics, Inc. No other potential conflict of interest relevant to this article was reported.

REFERENCES

1. Mankoff DA. A definition of molecular imaging. *J Nucl Med.* 2007;48(6):18N, 21N.
2. Wei W, Rosenkrans ZT, Liu J, Huang G, Luo QY, Cai W. ImmunoPET: concept, design, and applications. *Chem Rev.* 2020;120:3787–3851.
3. Chakravarty R, Goel S, Cai W. Nanobody: the "magic bullet" for molecular imaging? *Theranostics.* 2014;4:386–398.
4. Rashidian M, Ploegh H. Nanobodies as non-invasive imaging tools. *Immunooncology Technol.* 2020;7:2–14.
5. Xavier C, Vaneycken I, D'Huyvetter M, et al. Synthesis, preclinical validation, dosimetry, and toxicity of ^{68}Ga-NOTA-anti-HER2 Nanobodies for iPET imaging of HER2 receptor expression in cancer. *J Nucl Med.* 2013;54:776–784.
6. Keyaerts M, Xavier C, Heemskerk J, et al. Phase I study of ^{68}Ga-HER2-Nanobody for PET/CT assessment of HER2 expression in breast carcinoma. *J Nucl Med.* 2016;57:27–33.
7. D'Huyvetter M, De Vos J, Xavier C, et al. ^{131}I-labeled anti-HER2 camelid sdAb as a theranostic tool in cancer treatment. *Clin Cancer Res.* 2017;23:6616–6628.
8. D'Huyvetter M, Vos J, Caveliers V, et al. Phase I trial of ^{131}I-GMIB-Anti-HER2-VHH1, a new promising candidate for HER2-targeted radionuclide therapy in breast cancer patients. *J Nucl Med.* 2021;62:1097–1105.
9. Feng Y, Meshaw R, McDougald D, et al. Evaluation of an ^{131}I-labeled HER2-specific single domain antibody fragment for the radiopharmaceutical therapy of HER2-expressing cancers. *Sci Rep.* 2022;12:3020.
10. Zhao L, Liu C, Xing Y, et al. Development of a ^{99m}Tc-labeled single-domain antibody for SPECT/CT assessment of HER2 expression in breast cancer. *Mol Pharm.* 2021;18:3616–3622.

11. Vaidyanathan G, McDougald D, Choi J, et al. Preclinical evaluation of ^{18}F-labeled anti-HER2 Nanobody conjugates for imaging HER2 receptor expression by immuno-PET. *J Nucl Med.* 2016;57:967–973.
12. Wang C, Chen Y, Hou YN, et al. ImmunoPET imaging of multiple myeloma with [^{68}Ga]Ga-NOTA-Nb1053. *Eur J Nucl Med Mol Imaging.* 2021;48:2749–2760.
13. Zhou Z, Meshaw R, Zalutsky MR, Vaidyanathan G. Site-specific and residualizing linker for ^{18}F labeling with enhanced renal clearance: application to an anti-HER2 single-domain antibody fragment. *J Nucl Med.* 2021;62:1624–1630.
14. Vosjan MJ, Perk LR, Roovers RC, et al. Facile labelling of an anti-epidermal growth factor receptor Nanobody with ^{68}Ga via a novel bifunctional desferal chelate for immuno-PET. *Eur J Nucl Med Mol Imaging.* 2011;38:753–763.
15. Gainkam LO, Huang L, Caveliers V, et al. Comparison of the biodistribution and tumor targeting of two ^{99m}Tc-labeled anti-EGFR nanobodies in mice, using pinhole SPECT/micro-CT. *J Nucl Med.* 2008;49:788–795.
16. Krüwel T, Nevoltris D, Bode J, et al. In vivo detection of small tumour lesions by multi-pinhole SPECT applying a ^{99m}Tc-labelled nanobody targeting the epidermal growth factor receptor. *Sci Rep.* 2016;6:21834.
17. Bensch F, van der Veen EL, Lub-de Hooge MN, et al. ^{89}Zr-atezolizumab imaging as a non-invasive approach to assess clinical response to PD-L1 blockade in cancer. *Nat Med.* 2018;24:1852–1858.
18. Hirsch FR, McElhinny A, Stanforth D, et al. PD-L1 immunohistochemistry assays for lung cancer: results from phase 1 of the blueprint PD-L1 IHC assay comparison project. *J Thorac Oncol.* 2017;12:208–222.
19. Xing Y, Chand G, Liu C, et al. Early phase I study of a ^{99m}Tc-labeled anti-programmed death ligand-1 (PD-L1) single-domain antibody in SPECT/CT assessment of PD-L1 expression in non-small cell lung cancer. *J Nucl Med.* 2019;60:1213–1220.
20. Lv G, Sun X, Qiu L, et al. PET imaging of tumor PD-L1 expression with a highly specific nonblocking single-domain antibody. *J Nucl Med.* 2020;61:117–122.
21. Yang Y, Wang C, Wang Y, et al. Dose escalation biodistribution, positron emission tomography/computed tomography imaging and dosimetry of a highly specific radionuclide-labeled non-blocking nanobody. *EJNMMI Res.* 2021;11:113.
22. Bridoux J, Broos K, Lecocq Q, et al. Anti-human PD-L1 Nanobody for immuno-PET imaging: validation of a conjugation strategy for clinical translation. *Biomolecules.* 2020;10:1388.
23. Li D, Cheng S, Zou S, et al. Immuno-PET Imaging of ^{89}Zr labeled anti-PD-L1 domain antibody. *Mol Pharm.* 2018;15:1674–1681.
24. Wei W, Zhang D, Wang C, et al. Annotating CD38 expression in multiple myeloma with [^{18}F]F-Nb1053. *Mol Pharm.* November 30, 2021 [Epub ahead of print].
25. Shi L, Chen B, Liu T, et al. ^{99m}Tc-CD3813: a Nanobody-based single photon emission computed tomography radiotracer with clinical potential for myeloma imaging and evaluation of CD38 expression. *Mol Pharm.* 2022; Epub ahead of print.
26. Wei W, Zhang Y, Zhang D, et al. Annotating BCMA expression in multiple myelomas. *Mol Pharm.* November 29, 2021 [Epub ahead of print].
27. De Veirman K, Puttemans J, Krasniqi A, et al. CS1-specific single-domain antibodies labeled with actinium-225 prolong survival and increase CD8+ T cells and PD-L1 expression in multiple myeloma. *OncoImmunology.* 2021;10:2000699.
28. Ghai A, Zheleznyak A, Mixdorf M, et al. Development of [^{89}Zr]DFO-elotuzumab for immunoPET imaging of CS1 in multiple myeloma. *Eur J Nucl Med Mol Imaging.* 2021;48:1302–1311.
29. Puttemans J, Stijlemans B, Keyaerts M, et al. The road to personalized myeloma medicine: patient-specific single-domain antibodies for anti-idiotypic radionuclide therapy. *Mol Cancer Ther.* 2022;21:159–169.
30. Duray E, Lejeune M, Baron F, et al. A non-internalised CD38-binding radiolabelled single-domain antibody fragment to monitor and treat multiple myeloma. *J Hematol Oncol.* 2021;14:183.
31. An S, Zhang D, Zhang Y, et al. GPC3-targeted immunoPET imaging of hepatocellular carcinomas. *Eur J Nucl Med Mol Imaging.* 2022;49:2682–2692.
32. van Lith SAM, Huizing FJ, Franssen GM, et al. Novel VHH-based tracers with variable plasma half-lives for imaging of CAIX-expressing hypoxic tumor cells. *Mol Pharm.* 2022; Epub ahead of print.
33. Liu T, Wu Y, Shi L, et al. Preclinical evaluation of [^{99m}Tc]Tc-labeled anti-EpCAM nanobody for EpCAM receptor expression imaging by immuno-SPECT/CT. *Eur J Nucl Med Mol Imaging.* 2022;49:1810–1821.
34. Demine S, Garcia Ribeiro R, Thevenet J, et al. A nanobody-based nuclear imaging tracer targeting dipeptidyl peptidase 6 to determine the mass of human beta cell grafts in mice. *Diabetologia.* 2020;63:825–836.
35. Balhuizen A, Massa S, Mathijs I, et al. A nanobody-based tracer targeting DPP6 for non-invasive imaging of human pancreatic endocrine cells. *Sci Rep.* 2017;7:15130.
36. Wei W, Jiang D, Ehlerding EB, Luo Q, Cai W. Noninvasive PET imaging of T cells. *Trends Cancer.* 2018;4:359–373.
37. Pandit-Taskar N, Postow MA, Hellmann MD, et al. First-in-humans imaging with ^{89}Zr-Df-IAB22M2C anti-CD8 minibody in patients with solid malignancies: preliminary pharmacokinetics, biodistribution, and lesion targeting. *J Nucl Med.* 2020;61:512–519.
38. Farwell MD, Gamache RF, Babazada H, et al. CD8-targeted PET imaging of tumor-infiltrating T cells in patients with cancer: a phase I first-in-humans study of ^{89}Zr-Df-IAB22M2C, a radiolabeled Anti-CD8 minibody. *J Nucl Med.* 2022;63:720–726.
39. Rashidian M, Ingram JR, Dougan M, et al. Predicting the response to CTLA-4 blockade by longitudinal noninvasive monitoring of CD8 T cells. *J Exp Med.* 2017;214:2243–2255.
40. Van Elssen CH, Rashidian M, Vrbanac V, et al. Noninvasive imaging of human immune responses in a human xenograft model of graft-versus-host disease. *J Nucl Med.* 2017;58:1003–1008.
41. Rothlauf PW, Li Z, Pishesha N, et al. Noninvasive immuno-PET imaging of CD8$^+$ T cell behavior in influenza a virus-infected mice. *Front Immunol.* 2021;12:777739.
42. Rashidian M, LaFleur MW, Verschoor VL, et al. Immuno-PET identifies the myeloid compartment as a key contributor to the outcome of the antitumor response under PD-1 blockade. *Proc Natl Acad Sci USA.* 2019;116:16971–16980.
43. Zhao H, Wang C, Yang Y, et al. ImmunoPET imaging of human CD8$^+$ T cells with novel ^{68}Ga-labeled nanobody companion diagnostic agents. *J Nanobiotechnology.* 2021;19:42.
44. Traenkle B, Kaiser PD, Pezzana S, et al. Single-domain antibodies for targeting, detection, and in vivo imaging of human CD4$^+$ cells. *Front Immunol.* 2021;12:799910.
45. Lecocq Q, Awad RM, De Vlaeminck Y, et al. Single-domain antibody nuclear imaging allows noninvasive quantification of LAG-3 expression by tumor-infiltrating leukocytes and predicts response of immune checkpoint blockade. *J Nucl Med.* 2021;62:1638–1644.
46. Blykers A, Schoonooghe S, Xavier C, et al. PET imaging of macrophage mannose receptor-expressing macrophages in tumor stroma using ^{18}F-radiolabeled camelid single-domain antibody fragments. *J Nucl Med.* 2015;56:1265–1271.
47. Xavier C, Blykers A, Laoui D, et al. Clinical translation of [^{68}Ga]Ga-NOTA-anti-MMR-sdAb for PET/CT imaging of protumorigenic macrophages. *Mol Imaging Biol.* 2019;21:898–906.
48. Varasteh Z, Mohanta S, Li Y, et al. Targeting mannose receptor expression on macrophages in atherosclerotic plaques of apolipoprotein E-knockout mice using ^{68}Ga-NOTA-anti-MMR nanobody: non-invasive imaging of atherosclerotic plaques. *EJNMMI Res.* 2019;9:5.
49. Broisat A, Hernot S, Toczek J, et al. Nanobodies targeting mouse/human VCAM1 for the nuclear imaging of atherosclerotic lesions. *Circ Res.* 2012;110:927–937.
50. De Vos J, Mathijs I, Xavier C, et al. Specific targeting of atherosclerotic plaques in ApoE(−/−) mice using a new camelid sdAb binding the vulnerable plaque marker LOX-1. *Mol Imaging Biol.* 2014;16:690–698.
51. Movahedi K, Schoonooghe S, Laoui D, et al. Nanobody-based targeting of the macrophage mannose receptor for effective in vivo imaging of tumor-associated macrophages. *Cancer Res.* 2012;72:4165–4177.
52. Senders ML, Hernot S, Carlucci G, et al. Nanobody-facilitated multiparametric PET/MRI phenotyping of atherosclerosis. *JACC Cardiovasc Imaging.* 2019;12:2015–2026.
53. Rashidian M, Keliher EJ, Bilate AM, et al. Noninvasive imaging of immune responses. *Proc Natl Acad Sci USA.* 2015;112:6146–6151.
54. Ackaert C, Smiejkowska N, Xavier C, et al. Immunogenicity risk profile of nanobodies. *Front Immunol.* 2021;12:632687.
55. Yang E, Liu Q, Huang G, Liu J, Wei W. Engineering nanobodies for next-generation molecular imaging. *Drug Discov Today.* 2022;27:1622–1638.
56. Molitoris BA, Sandoval RM, Yadav SPS, Wagner MC. Albumin uptake and processing by the proximal tubule: physiologic, pathologic and therapeutic implications. *Physiol Rev.* 2022;102:1625–1667.
57. Arano Y. Renal brush border strategy: a developing procedure to reduce renal radioactivity levels of radiolabeled polypeptides. *Nucl Med Biol.* 2021;92:149–155.
58. D'Huyvetter M, Vincke C, Xavier C, et al. Targeted radionuclide therapy with a ^{177}Lu-labeled anti-HER2 nanobody. *Theranostics.* 2014;4:708–720.
59. Hofstrom C, Orlova A, Altai M, Wangsell F, Graslund T, Tolmachev V. Use of a HEHEHE purification tag instead of a hexahistidine tag improves biodistribution of affibody molecules site-specifically labeled with ^{99m}Tc, ^{111}In, and ^{125}I. *J Med Chem.* 2011;54:3817–3826.
60. Gainkam LO, Caveliers V, Devoogdt N, et al. Localization, mechanism and reduction of renal retention of technetium-99m labeled epidermal growth factor receptor-specific nanobody in mice. *Contrast Media Mol Imaging.* 2011;6:85–92.
61. Baudhuin H, Van Bockstal PJ, De Beer T, et al. Lyophilization of NOTA-sdAbs: first step towards a cold diagnostic kit for ^{68}Ga-labeling. *Eur J Pharm Biopharm.* 2021;166:194–204.
62. Langbein T, Weber WA, Eiber M. Future of theranostics: an outlook on precision oncology in nuclear medicine. *J Nucl Med.* 2019;60(suppl 2):13S–19S.
63. Feng Y, Meshaw R, Zhao XG, Jannetti SA III, Vaidyanathan G, Zalutsky MR. Effective treatment of human breast carcinoma xenografts with single-dose ^{211}At-labeled Anti-HER2 single domain antibody fragment. *J Nucl Med.* May 26, 2022 [Epub ahead of print].